

Climate change enhances interannual variability of the Nile river flow

Mohamed S. Siam* and Elfatih A. B. Eltahir

The human population living in the Nile basin countries is projected to double by 2050, approaching one billion¹. The increase in water demand associated with this burgeoning population will put significant stress on the available water resources. Potential changes in the flow of the Nile River as a result of climate change may further strain this critical situation^{2,3}. Here, we present empirical evidence from observations and consistent projections from climate model simulations suggesting that the standard deviation describing interannual variability of total Nile flow could increase by 50% ($\pm 35\%$) (multi-model ensemble mean ± 1 standard deviation) in the twenty-first century compared to the twentieth century. We attribute the relatively large change in interannual variability of the Nile flow to projected increases in future occurrences of El Niño and La Niña events^{4,5} and to observed teleconnection between the El Niño–Southern Oscillation and Nile River flow^{6,7}. Adequacy of current water storage capacity and plans for additional storage capacity in the basin will need to be re-evaluated given the projected enhancement of interannual variability in the future flow of the Nile river.

The Nile river basin is an ecosystem under severe stress. The basin is shared by about 400 million people in eleven countries with economies that depend heavily on agriculture, which employs the vast majority of the labour force in most of these countries¹. Furthermore, almost half of the Nile basin countries are projected to live below the water scarcity level, 1,000 m³/person/year, by 2030^{8,9}. Thus, any future changes in the magnitude of the flow volume of the Nile river can lead to significant impacts on the lives of people living within the basin and may increase the already high level of water stress.

To fully utilize the water resources of the basin, several dams were built in the previous century to control the seasonal and interannual variability of the Nile flow. The recent conflict over the Nile water has received significant attention in the past few years after the decision by Ethiopia to build a large dam on the Blue Nile (the Grand Ethiopian Renaissance Dam, or GERD) to produce electricity, mostly for export to neighbouring countries. The dam, currently under construction, is relatively large compared to previous designs for the same location, which raised serious concerns regarding its effect on water shares of downstream countries (that is, Egypt and Sudan). If variability of the Nile flow changes in the future, then water storage capacity in the basin will need to be re-evaluated.

Until recently, attempts to project the future of the Nile flow yielded inconsistent results. Although several studies examined the impacts of climate change on the Nile basin using different approaches^{10–18}, the uncertainty surrounding conclusions from these studies was high for several reasons. First, none of the previous studies presented observational evidence to support their hypotheses, as they estimated the impacts of climate change on the flow of Nile

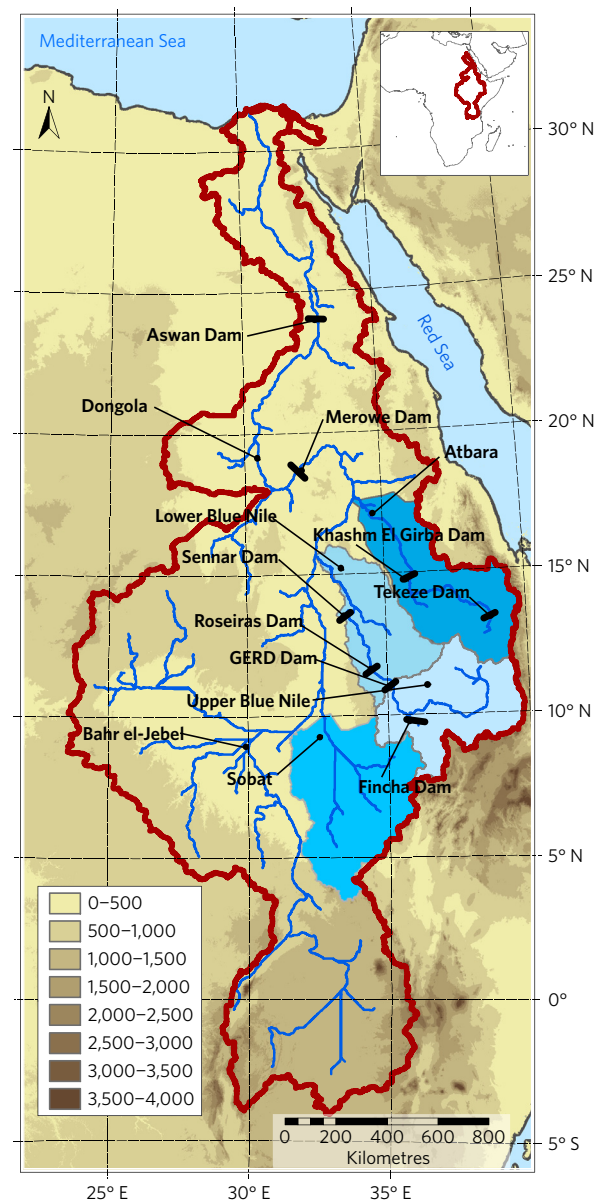


Figure 1 | Topographic map of Eastern Africa and the Nile sub-basins. Topographic map of Eastern Africa showing the main tributaries of Nile basins (Upper Blue Nile, Sobat, Atbara and Bahr el-Jebel) and different dams in these basins. The rainfall and runoff data analysed in this paper are averaged over the Upper Blue Nile, Sobat and Atbara basins.

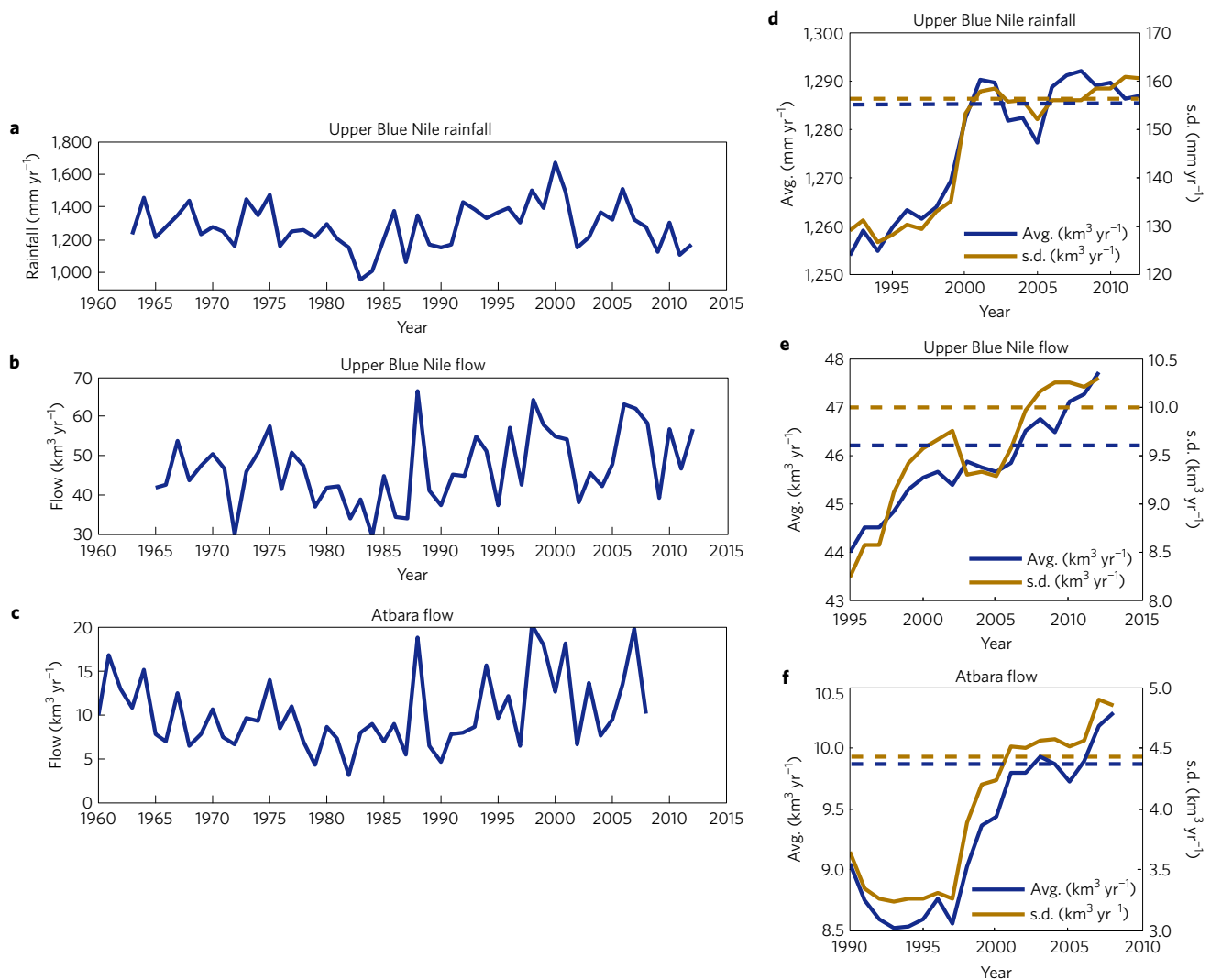


Figure 2 | Observed stream flows and rainfall, and moving averages for the mean and standard deviation for the Upper Blue Nile and Atbara basins.

a, Time series of the annual rainfall based on the weighted average of rainfall stations over the Upper Blue Nile basin (see Supplementary Methods). **b,c**, Time series of the annual stream flow averaged between June and May for the Upper Blue Nile and Atbara basins, respectively. **d**, 30-year moving average for the rainfall mean and standard deviation of the Upper Blue Nile. **e,f**, 30-year moving average for the stream flow mean and standard deviation of the Upper Blue Nile and Atbara basins respectively. In **d-f**, the dashed lines in blue and brown are the 90% confidence levels of the mean and standard deviation using the t-test and Chi-square distributions, respectively, based on the mean and standard deviation of the periods 1965–1995 and 1960–1990 for the Upper Blue Nile and Atbara, respectively. In **d-f** the moving average is plotted at the last year of the 30 years.

river only using Global Climate Models (GCMs) without presenting recent observations that show similar trends. Second, no consistent physical mechanism was advanced to explain the future changes. Third, wide disagreement persists between the results of simulations using the GCMs, not only in magnitude but also in the sign of projected changes in rainfall over the basin^{2,3}. These combined factors made it difficult to reach a consensus on the impact of climate change on the Nile river flow. Here, we use recent observations and climate models simulations to support the hypothesis that both the long-term mean and interannual variability of the Nile river flow may increase due to climate change.

The Nile river basin has four main tributaries: the Upper Blue Nile, Atbara, Sobat and Bahr el-Jebel (Fig. 1). The Upper Blue Nile is responsible for almost 56% of the total Nile flow, and each of Sobat and Atbara adds about 12% of the total flow at Dongola¹⁹ (Fig. 1). In this study, we focus on the Upper Blue Nile, Sobat and Atbara, hereinafter referred to as the Eastern Nile basin, as they represent almost 80% of the total Nile flow at Dongola (Fig. 1). The flows and rainfall patterns (that is, long-term mean and standard deviation) of

the Upper Blue Nile, Sobat and Atbara have been changing over the past 50 years (Fig. 2a–c). These changes are reflected in the 30-year moving averages of the mean and standard deviation of annual river flow and annual rainfall, as they both persistently increase with time (Fig. 2d–f). The increase of variability in the flow of Nile sub-basins during the past 50 years is also consistent with changes in variability of the longer record describing main Nile flow at Dongola. The 30-year moving average of the coefficient of variation of the flow at Dongola has been increasing since 1940 following a previous peak in variability around the 1920s (Fig. 3c).

The observed increases in the mean and standard deviation are projected to persist during the twenty-first century, as evident in the runoff simulated by the GCMs (indicated by the multi-model ensemble average, thick red line, Fig. 3a,b,d and Supplementary Figs 1 and 2). The runoff simulated by the GCMs was bias-corrected (see Methods section) to minimize the impact of discrepancies between simulations and observations. The long-term mean and standard deviation of total annual river flow are expected to increase by almost 15% and 50%, respectively, for the twenty-first century

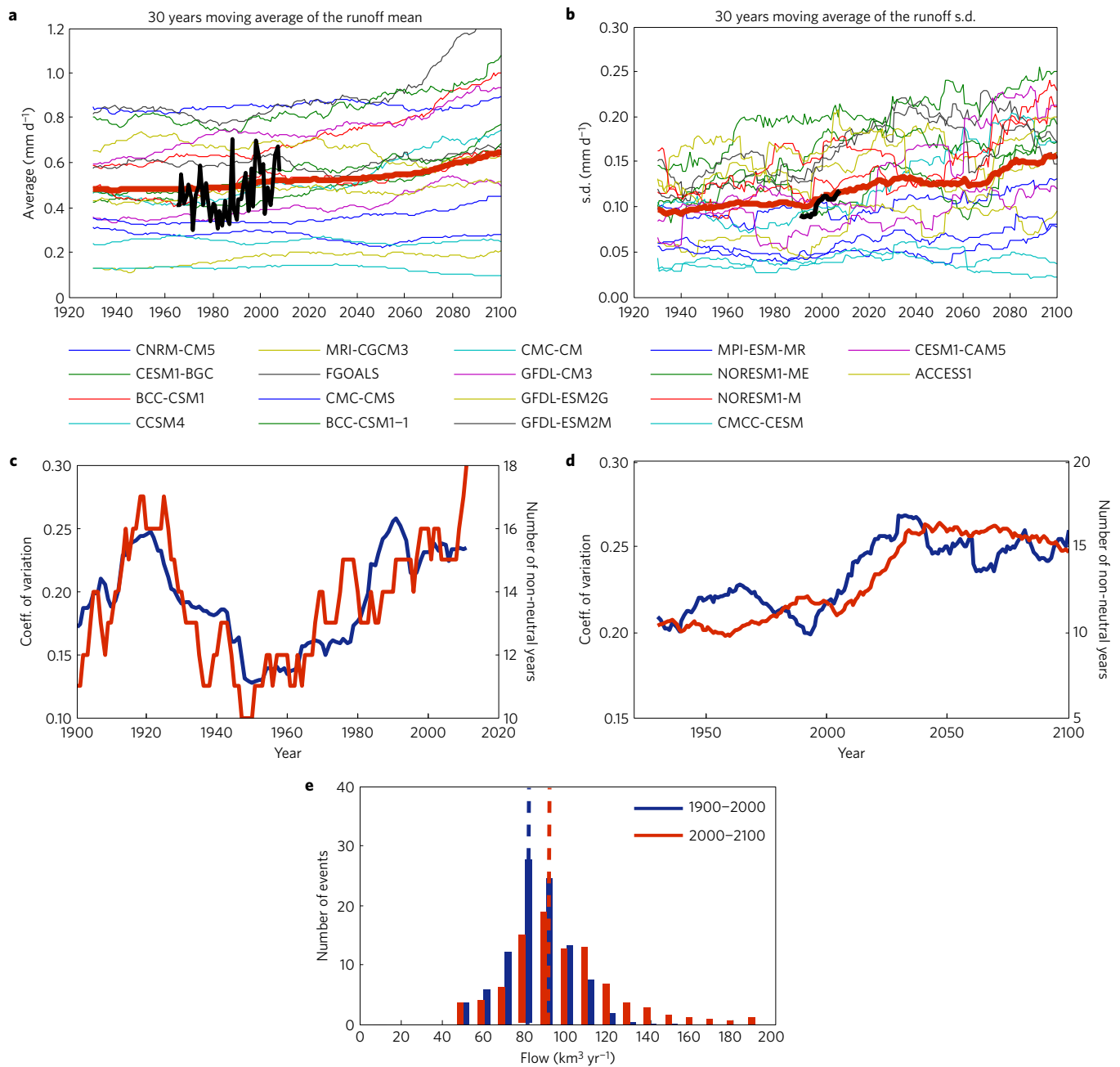


Figure 3 | Changes in moving averages for the mean and standard deviation, coefficient of variation, number of ENSO events and frequency distribution of flow over Eastern Nile basin using 18 CMIP5 GCMs. a,b, 30-year moving averages of the mean and standard deviation of the runoff simulated by the models from 1900 to 2100, the 95% confidence levels of the mean and standard deviation using Student’s *t* and Chi-square tests are 0.54 (mm d^{-1}) and 0.11 (mm d^{-1}), respectively, based on the mean and standard deviation of the period (1900–1930). The thick black line is the observed annual flow of Atbara and Upper Blue Nile in **a**, and the 30-year moving average of the standard deviation of the flow of Atbara and Upper Blue Nile basin in **b**. The Sobat flows are not included as they were not available. **c**, 30-year moving average of the coefficient of variation (blue line) of the stream flow at Dongola with the number of non-neutral years (red line) (that is, moderate and extreme El Niño and La Niña years). **d**, 30-year moving average of ensemble average of the coefficient of variation (blue line) of 18 GCMs of the runoff of the Eastern Nile basin with the number of non-neutral years (red line) (that is, moderate and extreme El Niño and La Niña years). **e**, Changes in the frequency distribution in future Nile flow based on bias correction approach (see Supplementary Methods). The change in the long-term average of annual Nile flow for the future period (2000–2100; red dashed lines) is statistically significant above the 95% confidence level using Student’s *t*-test compared the past period (1900–2000; blue solid lines). In **a–d** the moving average is plotted at the last year of the 30 years.

compared to the twentieth century. Hence, we conclude that the projected relative change in interannual variability is significantly larger than the corresponding change in long-term mean flow. This conclusion is consistent with the magnitudes of the changes that has already been observed in the Nile river flow (see Fig. 2). These

changes in the mean and variability in the annual flow of Nile river are also evident in the projected change in the frequency distribution of the annual Nile flow. The distribution of the flow in the twentieth century is closely clustered around the mean, with few extreme events (that is, below $70 \text{ km}^3 \text{ yr}^{-1}$ and higher than

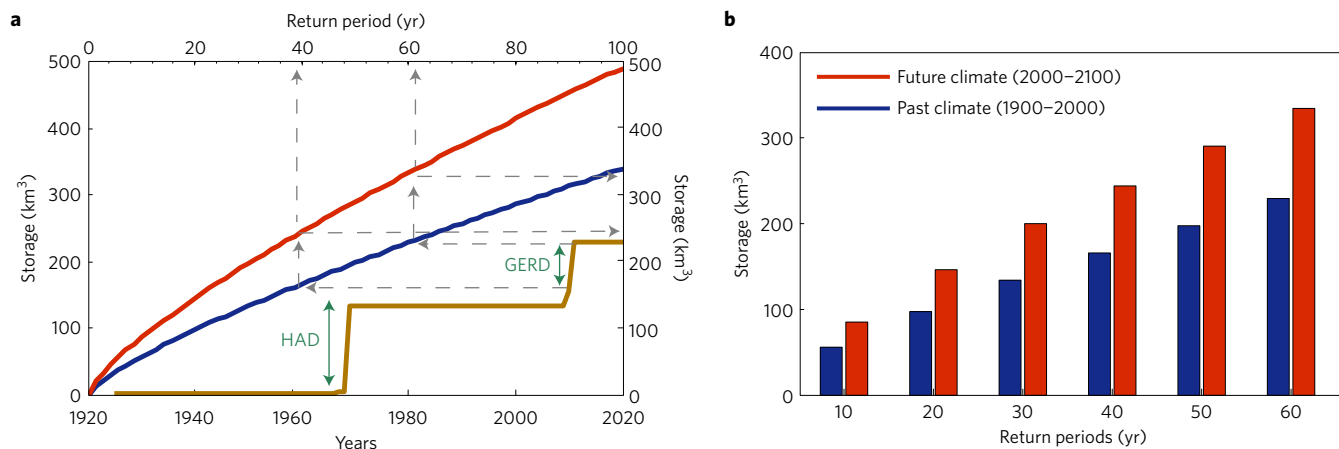


Figure 4 | Total current water storage in the Eastern Nile basin, and required changes in future storage to accommodate the effects of climate change.

a, The estimated water storage as a function of the return period based on the Hurst equation; the blue and red lines are for the past climate (1900–2000) and future climate (2000–2100) periods, respectively (see Water Storage Analysis in Methods) and the increase in water storage capacity of the dams in the Eastern Nile basin with time including Sennar, Khashm El Girba, Roseiras, High Aswan Dam (HAD), Fincha, Meroewe, Tekeze and the Grand Ethiopian Renaissance Dam (GERD; to be completed by 2017). **b**, Water storage required for different return periods according to the Hurst equation for the past climate (1900–2000) and future climate (2000–2100) periods.

100 km³ yr⁻¹), whereas the future flows have fewer normal events (that is, between 70 km³ yr⁻¹ and 100 km³ yr⁻¹) and more high flow events (that is, greater than 100 km³ yr⁻¹) (Fig. 3e). To study the sensitivity of our conclusions to the choice of the climate models, the projected changes in the Nile flow are estimated using different combinations of climate models (Supplementary Information). Our conclusions remain the same regardless of which combination of models is chosen to estimate the trends in the mean or variance (Supplementary Figs 8 and 9 and Supplementary Table 8).

The projected increase in the interannual variability of the flow of the Nile river, as shown in the observed stream flows of the major tributaries and simulated runoff of the GCMs, is consistent with the increase in the frequencies of El Niño and La Niña events projected by recent studies^{4,5} (Supplementary Fig. 4a). These changes in the frequencies of El Niño and La Niña events would change the Nile flow patterns following the observed teleconnection between ENSO and the Nile, in which El Niño and La Niña events induce low and high flows in the river, respectively^{20–22} (Fig. 3d and Supplementary Fig. 4b). It is also important to note that the increase in the variability in the flow of the Nile flow occurs between 2010 and 2040 and then stabilizes until the end of the twenty-first century, which is consistent with the weakening of the Walker circulation during the same period (2010–2040)²³. Although ENSO is a major driver of interannual variability in the Nile flow, and the tropical climate in general, this oscillation explains only 27% of the observed natural variability, as shown in Supplementary Fig. 4b. In a different approach to the same problem, we use the ENSO–Nile teleconnection to predict future Nile flow based on changes in frequency of El Niño and La Niña events projected by an ensemble of GCMs. The future Nile flows estimated based on future El Niño and La Niña events exhibit the same changes in the mean, interannual variability and frequency distribution as the simulated runoff by the GCMs (see Sampling Analysis in Methods and Supplementary Fig. 4c,d). The agreement between the changes in the future flows projected using these two different approaches (that is, simulated flow by the GCMs; and based on projected changes in El Niño and La Niña events) increases our confidence in the projected changes and support the mechanism proposed to explain the future changes in the Nile flows. Moreover, a sensitivity analysis of the results based on the choice of the GCMs using the sampling approach is conducted and the results are consistent regardless of which combination of models results is chosen to

estimate the changes in the flow of the Nile (Supplementary Fig. 10 and Supplementary Table 8). Our approach which emphasizes the teleconnection between ENSO and the Nile flow and our choice to use only GCMs that accurately simulate the statistics of ENSO resulted in narrowing the range of uncertainty about future Nile flow, and increasing our confidence in the projected impacts of climate change.

The relatively large increase in interannual variability in the flow of Nile river dictates an increase of almost 33% in the total storage capacity (from 340 to 460 km³) that is needed to maintain a flow in each year, for over 100 years, equivalent to the long-term mean flow (Fig. 4a) (see Methods for details of the Hurst storage analysis^{24,25}). It is also important to note that the long-term mean flow for the past (1900–2000) was about 80 km³ yr⁻¹, while the mean flow for the future (2000–2100) is projected to be about 92 km³ yr⁻¹. The current total storage capacity in the Eastern Nile river basin is about 155 km³ and is expected to increase to 230 km³ if the GERD is built (Fig. 4a). Based on our analysis shown in Fig. 4a, applying the Hurst equation, the current storage in the basin is sufficient for securing a yield equivalent to the observed mean annual flow, for about 40 years. To secure a yield equivalent to the projected mean annual flow for a similar 40 years into the future, the storage will have to be expanded by about 55%. However, after GERD is built, the new storage in the basin will be sufficient for securing a yield equivalent to the observed flow, for about 60 years (Fig. 4a). To secure a yield equivalent to the projected mean flow for a similar 60 years into the future, the storage will have to be expanded by about 45% (Fig. 4b) (it is important to note that our analysis does not include evaporation losses from new reservoirs behind dams).

Here, we project that the future water storage capacity in the basin needs to be re-evaluated to control the enhanced interannual variability in the flow and to capture the additional flow due to climate change. However, this increase in storage capacity may or may not be feasible, depending on several factors, including availability of suitable sites for dams, economic considerations, and agreement between Nile basin countries. Moreover, detailed studies for these new dams that identify the potential locations, sizes, operational rules and impacts on the water resources shares between riparian countries based on a range of expected changes in the future flows of the Nile will be required^{26,27}.

The lack of consensus between the past studies that investigated the impacts of climate change on the Nile river flow hinders the

development of effective climate change adaptation plans. Hence, knowledge about the future flow of the Nile river is needed to guide water resources planning, including proposals for dams and hydropower projects (for example, GERD). Based on our analysis using two different approaches and several different combinations of GCMs results, we project that the mean and interannual variability of annual flow in the Nile river basin will increase due to climate change. The projected increase in the interannual variability may limit the benefits of projected increase in mean flow, and hence motivate a significant increase in the water storage capacity to fully utilize the additional water resource. Future climate projections discussed here assume a business-as-usual scenario of greenhouse gas emissions. Any effective mitigation efforts are likely to impact these projections, and hence reduce the intensity of the projected impacts.

Methods

Methods, including statements of data availability and any associated accession codes and references, are available in the [online version of this paper](#).

Received 6 May 2016; accepted 17 March 2017;
published online 24 April 2017

References

1. *World Population Prospects: The 2012 Revision, Highlights and Advance Tables* Working Paper No. ESA/P/WP.228 (United Nations, Department of Economic and Social Affairs, Population Division, 2013).
2. Christensen, J. H. *et al.* in *Climate Change 2007: The Physical Science Basis* (eds Solomon, S. *et al.*) 847–940 (IPCC, Cambridge Univ. Press, 2007).
3. Christensen, J. H. *et al.* in *Climate Change 2013: The Physical Science Basis* (eds Stocker, T. F. *et al.*) 1217–1308 (IPCC, Cambridge Univ. Press, 2013).
4. Cai, W. *et al.* Increasing frequency of extreme El Niño events due to greenhouse warming. *Nat. Clim. Change* **4**, 111–116 (2014).
5. Cai, W. *et al.* Increased frequency of extreme La Nina events under greenhouse warming. *Nat. Clim. Change* **5**, 132–137 (2015).
6. Eltahir, E. A. B. El Niño and the natural variability in the flow of the Nile River. *Wat. Resour. Res.* **32**, 131–137 (1996).
7. Siam, M. S., Wang, G., Demory, M. E. & Eltahir, E. A. B. Role of the Indian Ocean sea surface temperature in shaping the natural variability in the flow of Nile River. *Clim. Dynam.* **43**, 1011–1023 (2014).
8. Baecher, G., Anderson, R., Britton, B., Brooks, K. & Gaudet, J. *The Nile Basin: Environmental Transboundary Opportunities and Constraints Analysis* (United States Agency for International Development, 2015).
9. *New Dimensions in Water Security: Water, Society and Ecosystem Services in the 21st century* (Food and Agriculture Organization of the United Nations, 2000).
10. Kim, U. & Kaluarachchi, J. J. Climate change impacts on water resources in the Upper Blue Nile River Basin, Ethiopia. *J. Am. Wat. Resour. Assoc.* **45**, 1361–1378 (2009).
11. Elshamy, M. E. Impacts of climate change on Blue Nile flows using bias corrected GCM scenarios. *Hydrol. Earth Syst. Sci.* **13**, 551–565 (2009).
12. Beyene, T., Lettenmaier, D. P. & Kabat, P. Hydrologic impacts of climate change on the Nile River Basin: implications of the 2007 IPCC scenarios. *Climatic Change* **100**, 433–461 (2009).
13. Yates, D. N. & Strzepek, K. M. An assessment of integrated climate change impacts on the agricultural economy of Egypt. *Climatic Change* **38**, 261–287 (1998).
14. Gebre, S. L. & Ludwig, F. Hydrological response to climate change of the upper Blue Nile River Basin: based on IPCC Fifth Assessment Report (AR5). *J. Climatol. Weath. Forecast.* **3**, 121 (2015).
15. Taye, M. T., Ntegeka, V., Ogiramo, N. P. & Willems, P. Assessment of climate change impact on hydrological extremes in two source regions of the Nile River Basin. *Hydrol. Earth Syst. Sci.* **15**, 209–222 (2011).
16. *Adaptation to Climate-change Induced Water Stress in the Nile Basin: A Vulnerability Assessment Report. Division of Early Warning and Assessment (DEWA)* (United Nations Environment Programme, 2013).
17. Conway, D. & Schipper, E. L. F. Adaptation to climate change in Africa: challenges and opportunities identified from Ethiopia. *Glob. Environ. Change* **21**, 227–237 (2011).
18. Conway, D. From headwater tributaries to international river: observing and adapting to climate variability and change in the Nile basin. *Glob. Environ. Change* **15**, 99–114 (2005).
19. Conway, D. & Hulme, M. Recent fluctuations in precipitation and runoff over the Nile subbasins and their impact on Main Nile discharge. *Climatic Change* **25**, 127–151 (1993).
20. Siam, M. S. & Eltahir, E. A. B. Explaining and forecasting interannual variability in the flow of the Nile River. *Hydrol. Earth Syst. Sci.* **19**, 1181–1192 (2015).
21. Wang, G. & Eltahir, E. A. B. Use of ENSO information in medium and long range forecasting of the Nile floods. *J. Clim.* **12**, 1726–1737 (1999).
22. ElDaw, A., Salas, J. D. & Garcia, L. A. Long range forecasting of the Nile river flows using climate forcing. *J. Appl. Meteorol.* **42**, 890–904 (2003).
23. Kim, S. T. *et al.* Response of El Niño sea surface temperature variability to greenhouse warming. *Nat. Clim. Change* **4**, 786–790 (2014).
24. Hurst, H. E., Black, R. P. & Simaika, Y. M. Long-term storage: an experimental study. *J. Roy. Stat. Soc. A* **129**, 591–593 (1966).
25. Hurst, H. E. Long term storage capacity of reservoirs. *Trans. Am. Soc. Civ. Eng.* **116**, 770–779 (1951).
26. Cervigni, R., Liden, R., Neumann, J. E. & Strzepek, K. M. (eds) *Enhancing the Climate Resilience of Africa's Infrastructure: The Power and Water Sectors* (World Bank Publications, 2015).
27. King, A. & Block, P. An assessment of reservoir filling policies for the Grand Ethiopian Renaissance Dam. *J. Wat. Clim. Change* **5**, 233–243 (2014).

Author contributions

E.A.B.E. conceived the study, and supervised the design and implementation of research. M.S.S. performed the analyses of observational data and climate models. E.A.B.E. supervised interpretation of results. M.S.S. wrote the paper, with input from E.A.B.E. Both authors contributed to revisions of the manuscript.

Additional information

Supplementary information is available in the [online version of the paper](#). Reprints and permissions information is available online at www.nature.com/reprints. Publisher's note: Springer Nature remains neutral with regard to jurisdictional claims in published maps and institutional affiliations. Correspondence and requests for materials should be addressed to M.S.S.

Competing financial interests

The authors declare no competing financial interests.

Methods

Bias correction using the probability matching method. The bias correction approach was used to correct for bias in hydrological variables in several previous studies^{11,28}. Here, the cumulative distribution function is calculated for the observed annual average Nile flow at Dongola for the past period (1900–2000). In the following step, the cumulative distribution function is calculated for the annual average simulated runoff by each GCM for the past period (1900–2000). Then, a set of bias correction factors are estimated by the ratio of the observed Nile flow at each cumulative probability to the corresponding Nile flow simulated by the GCM at that same cumulative probability. In other words, for each range of simulated Nile flow values produced by a GCM, we estimate a correction factor that would effectively match the observed and simulated probability distributions of past flows. For the period (2000–2100), the simulated runoff by each GCM is bias-corrected by multiplying the GCM simulated value by the corresponding correction factor.

Sampling analysis. In the sampling approach, we estimate the Nile flow based on the frequency of occurrence of different types of El Niño and La Niña events (that is, extreme El Niño, moderate El Niño, neutral, extreme La Niña and moderate La Niña). First, we compute the frequency of different events based on sea surface temperature (SST) observations using HadISST²⁹ for the period (1900–2000). The identification process of the different types of events follows the methodology of previous studies that were investigating the changes in the frequencies of El Niño and La Niña events^{4,5}. In these studies, the extreme El Niño events are identified when the average (December–February) rainfall over the Niño 3 region is greater than 5 mm d^{-1} . However, we replaced this condition by satisfying a SST condition over Niño 3 as there is no observed precipitation data available over the oceans for the whole period (1900–2000). It is estimated that when the rainfall over Niño 3 exceeds 5 mm d^{-1} , the average SST anomalies during December to February over Niño 3 are greater than 1.75 times the standard deviation. Thus, extreme El Niño events are identified when the (December–February) SST anomalies over Niño 3 are greater than 1.75 times the standard deviation. On the other hand, the extreme La Niña events are identified when the average (December–February) SST anomalies over Niño 4 are less than 1.75 times the standard deviation. The moderate El Niño events are identified when the average (December–February) SST anomalies over Niño 3 are greater than 0.5 times the standard deviation and less than 1.75 times the standard deviation. The moderate La Niña events are identified when the average (December–February) SST anomalies over Niño 4 are less than 0.5 and greater than 1.75 times the standard deviation. The remainder of events are considered as neutral events.

Second, for each type of event (that is, extreme El Niño, moderate La Niña, neutral, extreme La Niña and moderate La Niña) within the past period (1900–2000), the corresponding observed total Nile flows at Dongola are identified and grouped together for each type.

The same identification process of the different types is repeated for GCMs simulations for the periods (1900–2000) and (2000–2100). The different types of events are identified for each model and for the past period (1900–2000). Each time the model simulates any event, a value is picked randomly from the group of the observed Nile flow values for this type of event and is assigned to be the

corresponding Nile flow. This step is repeated for the future period (2000–2100); however, the magnitude of assigned flow is modified by the ratio of the simulated future runoff over ENB for that type of event in the period (2000–2100) to the past simulated runoff over ENB for the same type of event in the period (1900–2000).

Water storage analysis. The storage capacity required to accommodate the variability in any river flow and to supply an equal flow each year (that is, the long-term average) over a certain period of time (N) can be calculated by taking the departures of the flow from the mean and summing these departures^{21,22}. Thus, the difference between the maximum and minimum of these continued sums is the required storage capacity. Several phenomenon, including the Nile flow, which have long time series follow a certain relation between the difference of maximum and minimum continued sum, the standard deviation (σ), and (N) (ref. 23). The relation has the form $R/\sigma = (N/2)^k$, where k is the Hurst coefficient²¹. The Hurst coefficient can be estimated by fitting the relation between (R/σ) and $(N/2)$ for different lengths of the time series of length (N). The summary of the changes in the 100-year storage and Hurst coefficients for the different GCMs is presented in Supplementary Table 7.

Data availability. In this study, we use several observational data sets and climate models simulations to investigate the future change in the interannual variability of the flow in the Nile river. The observational data sets include stream flow data at Dongola available from the Global River Discharge Database (GRDD)³⁰, stream flow data for Atbara and Upper Blue Nile basins available through personal communications with the ministries of water in the countries of the Nile basin, and rainfall data based on rain gauges from the Global Historical Climatology Network (GHCN-V2) (ref. 31). The climate models simulations are based on 18 GCMs that participated in the Coupled Model Inter-comparison Project Phase 5 (CMIP5) with the Representative Concentration Pathway (RCP 8.5) for future greenhouse gases projected emissions³². For further details about these data, please refer to sections 1 and 2 of the Supplementary Information. The data that support the findings of this study are available from the corresponding author upon request.

References

28. Yamana, T. K. *Mechanistic Modelling of the Links between Environment, Mosquitoes and Malaria Transmission in the Current and Future Climates of West Africa* (Doctoral dissertation, Massachusetts Institute of Technology, 2015).
29. Rayner, N. A. *et al.* Global analyses of sea surface temperature, sea ice, and night marine air temperature since the late nineteenth century. *J. Geophys. Res.* **108**, 4407 (2003).
30. Vorosmarty, C. J., Fekete, B. M. & Tucker, B. A. *Global River Discharge 1807–1991* Version. 1.1 (RivDIS). Data set. (Oak Ridge National Laboratory Distributed Active Archive Center, 1998); <http://www.daac.ornl.gov>
31. Vose, R. S. *et al.* *Global Historical Climatology Network 1753–1990* (ORNL DAAC, 2016); <http://dx.doi.org/10.3334/ORNLDAAC/220>
32. Taylor, K. E., Stouffer, R. J. & Meehl, G. A. An overview of CMIP5 and the experiment design. *Bull. Am. Meteorol. Soc.* **93**, 485–498 (2015).